

MOL #66613

μ - Opioid receptors: correlation of agonist efficacy for signalling with ability to activate internalization

Jamie McPherson, Guadalupe Rivero, Myrna Baptist, Javier Llorente, Suleiman Al-Sabah¹, Cornelius Krasel², William L Dewey, Chris P Bailey, Elizabeth M Rosethorne, Steven J Charlton , Graeme Henderson, and Eamonn Kelly

Department of Physiology and Pharmacology, University of Bristol, Bristol, United Kingdom (J.M., G.R., M.B., J.L., G.H., E.K.); School of Pharmacy, University of Reading, Whiteknights, United Kingdom (S.A., C.K.); Department of Pharmacology and Toxicology, Virginia Commonwealth University Medical Center, Richmond, VA (W.L.D.); Department of Pharmacy and Pharmacology, University of Bath, Claverton Down, Bath, United Kingdom (C.P.B.) and Novartis Institutes for Biomedical Research, Horsham, West Sussex, United Kingdom (E.M.R., S.J.C.).

MOL #66613

Running Title: Relative operational efficacy of μ -opioid receptor agonists

*Correspondence should be addressed to: Dr Eamonn Kelly, Department of Physiology and Pharmacology, School of Medical Sciences, University of Bristol, Bristol, BS8 1TD, UK.

Email: E.Kelly@bristol.ac.uk

Tel: + 44 1173311402

Fax: +44 1173312288

Number of text pages: 44

Number of figures: 5 (plus 1 Supplemental data File containing 6 Figs)

Number of tables: 2

Word count:

Abstract: 182

Introduction: 746

Discussion: 1498

Abbreviations:

aCSF, artificial cerebrospinal fluid; BSA, Bovine Serum Albumin; DAMGO, [D-Ala², N-MePhe⁴, Gly-ol]-enkephalin; DMEM, Dulbecco's modified Eagle's medium; EA, Enzyme Acceptor; CFP, enhanced Cyan Fluorescent Protein; YFP, enhanced Yellow Fluorescent Protein; ELISA, enzyme-linked immunosorbent assay; K_D, equilibrium dissociation constant; FRET, Fluorescence Resonance Energy Transfer; GPCR, G protein-coupled receptor; GRK2, G protein coupled receptor kinase 2; HBBS, Hank's buffered saline solution; HEK293, Human embryonic kidney 293 cells; 6 MAM, 6-monoacetylmorphine; M6G, morphine-6-glucuronide; MOPr, μ opioid receptor; PBS, phosphate buffered saline; RAVE, Relative Activity Versus Endocytosis; SDS-PAGE, sodium dodecyl sulphate-polyacrylamide gel electrophoresis.

MOL #66613

ABSTRACT

We have compared the ability of a number of μ -opioid receptor (MOPr) ligands to activate G proteins with their abilities to induce MOPr phosphorylation, to promote association of arrestin-3 and to cause MOPr internalization. For a model of G protein-coupled receptor (GPCR) activation where all agonists stabilize a single active conformation of the receptor, a close correlation between signalling outputs might be expected. Our results show that overall there is a very good correlation between efficacy for G protein activation and arrestin-3 recruitment, whilst a few agonists, in particular endomorphin 1 and endomorphin 2, display apparent bias towards arrestin recruitment. The agonist-induced phosphorylation of MOPr at Serine³⁷⁵, considered a key step in MOPr regulation, and agonist-induced internalization of MOPr were each found to correlate well with arrestin-3 recruitment. These data indicate that for the majority of MOPr agonists the ability to induce receptor phosphorylation, arrestin-3 recruitment and internalization can be predicted from their ability as agonists to activate G proteins. For the prototypic MOPr agonist morphine, its relatively weak ability to induce MOPr internalization can be explained by its low agonist efficacy.

MOL #66613

INTRODUCTION

Drugs such as morphine, that are agonists at the MOPr, are of great therapeutic importance in the management of pain and are also highly significant in terms of their abuse potential. MOPr agonists also induce the phenomenon of tolerance whereby increasing doses of the agonist are required to maintain the analgesic or euphoric effect of the drug (Corbett et al., 2006). A number of mechanisms have been proposed to mediate tolerance to opioid agonists (Williams et al., 2001), and in recent years there has been increased focus on the molecular regulation of MOPr as a mechanism of tolerance, in particular with regard to MOPr desensitization and internalization (for reviews see Connor et al., 2004; Bailey and Connor, 2005; Kelly et al., 2007; Koch and Holtt, 2008; Christie 2008). Although for some GPCRs there seems to be a clear correlation between agonist efficacy and the ability to induce receptor regulatory processes/mechanisms such as phosphorylation and desensitization, the situation for the MOPr is much less clear, with some evidence indicating that low efficacy agonists such as morphine are better able to induce tolerance than some higher efficacy agonists (Duttaroy and Yoburn 1995; Greksch et al., 2006).

A number of theories have been developed in an attempt to explain these observations (Bailey et al., 2006; Martini and Whistler, 2007; Koch and Holtt, 2008). For example, it has been proposed that MOPr agonists with relatively low efficacy are able to induce profound tolerance because they induce MOPr desensitization but little MOPr internalization such that the receptor is unable to undergo efficient dephosphorylation and resensitization as would occur with a

MOL #66613

higher efficacy internalizing agonist (Schulz et al., 2004). Alternatively we have shown that morphine and [D-Ala², N-MePhe⁴, Gly-ol]-enkephalin (DAMGO) induce MOPr desensitization by different molecular mechanisms (Johnson et al., 2006; Bailey et al., 2006; Bailey et al., 2009a; Bailey et al., 2009b), which could also explain the differing abilities of MOPr agonists to induce or maintain tolerance (Bailey et al., 2006; Hull et al., 2010). A further idea is that the low efficacy of morphine induces little MOPr desensitization and that it is instead the prolonged signalling of the morphine-activated receptor that leads to neuronal adaptations that precipitate tolerance (Whistler et al., 1999). Such ideas have formed the basis of theories of opioid tolerance, such as the Relative Activity Versus Endocytosis (RAVE) theory, but these remain the subject of conjecture (see for example Martini and Whistler, 2007; Koch and Holtt, 2008).

An important element in the analysis of opioid tolerance is the ability to obtain accurate measurements of agonist efficacy. However since this property is both a drug- and tissue-dependent quantity, its value for an agonist can vary from tissue to tissue (Christopoulos and El-Fakahany, 1999), which can confound interpretation. For example, some opioid agonists are full agonists in clonal cell lines expressing high levels of MOPr but may be partial agonists in neurones where MOPr expression is lower and a receptor reserve may not exist (Selley et al., 1998). Perhaps a more useful measure of efficacy is relative intrinsic efficacy (Furchgott and Bursztyn, 1967), which enables comparison of responses produced by equivalent fractional occupancy of the receptors by different agonists in the same tissue. In this case the tissue factors contributing to efficacy

MOL #66613

cancel out and the relative intrinsic efficacy thus becomes a measurement of the relative abilities of different agonists to activate the receptor. Operational analysis of agonist responses (Black and Leff, 1983) provides one means of determining the relative intrinsic efficacy of agonists. In this approach the operational efficacies (τ values) of a series of agonists in a particular cell type or tissue are determined from the concentration-effect data and can be used as a measure of agonist relative intrinsic efficacy (Black and Leff, 1983).

In the present study we have used operational analysis to determine the τ values of twenty-two opioid agonists for two signalling outputs of MOPr: G protein activation and non-visual arrestin recruitment. To achieve this we have employed high-throughput assay technology to construct full concentration-effect curves for MOPr agonist-induced [³⁵S]GTP γ S binding to cell membranes and arrestin-3 recruitment to MOPr in intact cells using the PathHunter™ assay system. In addition, we have measured the ability of a number of opioid agonists to induce phosphorylation of the MOPr at Serine³⁷⁵ and to cause MOPr internalization.

Correlation of these measures indicates that for the majority of MOPr agonists there is a good correlation between operational efficacy for G protein activation and activation of the MOPr internalization process.

MOL #66613

Materials and Methods

Cell culture and transfections. HEK293 cells were maintained at 37°C in 95% O₂, 5% CO₂, in Dulbecco's modified Eagle's medium (DMEM; Invitrogen, Carlsbad, CA) supplemented with 10% fetal bovine serum, 10 U/mL penicillin and 10 mg/ml streptomycin. In addition, the culture medium for the HEK293 cells stably expressing T7-tagged MOPr (Bailey et al., 2003; Rodriguez-Martin et al., 2008) contained 250 µg/ml of the selective antibiotic geneticin (PAA, Pasching, Austria).

The PathHunter™ β-arrestin assay (DiscoverX) uses enzyme fragment complementation between two portions of β-galactosidase to measure recruitment of β-arrestin to a GPCR after activation. The larger portion, the Enzyme Acceptor (EA) tag is fused to arrestin-3, and the smaller portion (ProLink™) is fused to the C-terminus of the GPCR of choice. Activation of the receptor causes recruitment of arrestin-3 to the GPCR thus forming a functional β-galactosidase enzyme, whose activity can be measured by the addition of a chemiluminescent substrate. The MOPr:ProLink™ receptor construct was stably expressed in HEK293 cells stably expressing arrestin-3:EA (DiscoverX, Birmingham, UK) using Lipofectamine ([Invitrogen](#), Paisley, UK) transfection according to manufacturer's instructions. Expression was maintained using antibiotic selection (250 µg/ml hygromycin; 500 µg/ml geneticin) and cells were passaged at 50 % confluency using trypsin/EDTA.

For Fluorescence Resonance Energy Transfer (FRET) experiments, the enhanced Cyan Fluorescent Protein (CFP) and enhanced Yellow Fluorescent

MOL #66613

Protein (YFP) (BD Biosciences Clontech, Heidelberg, Germany) constructs were fused to the COOH-terminus of bovine arrestin-3 and the rat MOPr respectively as previously described (Krasel et al., 2005). Briefly, the stop codon for each protein was replaced with an XbaI site (TCTAGA), and the coding sequences of CFP and YFP were appended in-frame. The pcDNA3-arrestin-3-CFP, pcDNA3-GRK2 and the pcDNA3-MOPr-YFP constructs were verified by sequencing. Transient transfection of HEK293 cells was carried out with Effectene (Qiagen, Hilden, Germany) if not otherwise indicated, 48 h before use. The ratio between MOPr-YFP DNA and arrestin-3-CFP DNA for transfection varied between 2:1 and 1:1.

[³⁵S]GTP γ S binding assay. The binding of [³⁵S]GTP γ S to membranes prepared from T7-MOPr-expressing cells was based on a previously described protocol (Johnson et al., 2006). Cells were grown to approximately 90% confluence, and removed from the culture flask using a lifting buffer (10 mM HEPES, 0.9% w/v NaCl, 0.2% w/v EDTA, pH 7.4) and cell scraper, pelleted by centrifugation (377g; 10 min) and resuspended in wash buffer 1 (10 mM HEPES, 10 mM EDTA, pH 7.4). The cell suspension was homogenised with an Ultra-Turrax disperser (5 \times 10 s bursts). The resulting homogenate was ultracentrifuged at 48,000g for 30 min at 4°C using a Beckman Avanti J-251 ultracentrifuge, the supernatant discarded and the pellet resuspended. This was repeated to wash, and the final pellet resuspended in wash buffer 2 (10 mM HEPES, 0.1 mM EDTA, pH 7.4) at a protein concentration of 3–5 mg/ml. Aliquots were flash frozen and maintained at -80°C until required.

MOL #66613

In some experiments [³⁵S]GTP γ S binding was also studied using membranes prepared from the HEK293 cells stably expressing epitope-tagged MOPr and arrestin-3 for the PathHunter™ assay. The procedure for membrane preparation was identical to that described above.

For the assay itself, 10 μ g of membrane protein was incubated in each well of a 96-well plate, diluted in a total volume of 250 μ l of Hank's buffered saline solution (HBSS; Invitrogen, Paisley, UK) containing 1 μ M GDP, 0.5 mg wheatgerm agglutinin Scintillation Proximity Assay beads (GE Healthcare, Little Chalfont, Bucks, UK), various concentrations of agonist and 300 pM [³⁵S]GTP γ S (1 mCi/ml; Perkin Elmer, Waltham, MA). On each plate a concentration-response curve to DAMGO was constructed and the data for all other agonists normalised to that obtained for DAMGO. Reactions were allowed to proceed for 1 h before plates were centrifuged at 1,500g for 2 min and scintillation was read on a TopCount scintillation counter (Perkin Elmer).

Arrestin translocation assay. HEK293 cells stably expressing arrestin-3 epitope-tagged with an EA moiety for the Pathhunter™ assay (DiscoverRx, Birmingham, UK) were stably transfected with the MOPr:ProLink™ receptor construct. For assays, the cells were plated the day preceding the assay at ~10,000 cells/well in 20 μ l volumes in a 384-well ViewPlate (Perkin Elmer). On the day of the assay, medium was removed and replaced with HBSS containing 0.1% Bovine Serum Albumin (BSA) and 20 mM HEPES, pH 7.4. Drugs were added in 5 μ l volumes to the wells, and left to incubate for 2 h at 22°C. Following incubation, 25 μ l of proprietary Flash reagent mixed with lysis buffer was added

MOL #66613

to each well using a Minitrak liquid handling system (Perkin Elmer), and luminescence was read after 3 min on a Leadseeker plate reader (GE Healthcare, Little Chalfont, Bucks, UK). Each concentration point had 4 replicates. Data were normalised relative to 30 μ M alfentanil and a buffer control.

Ligand binding assay. Membranes were prepared as for the [³⁵S]GTP γ S binding assay. For saturation binding experiments, [³H]-naloxone (1 mCi/ml; Perkin Elmer) was serially diluted 1:2 in HBSS/20 mM HEPES/pH 7.4 from 60 nM down to 30 pM. Next, 10 μ g of membrane protein was added to each well of a 96-well deep well plate containing radioligand and HBSS/20 mM HEPES/pH 7.4, with a total reaction volume of 500 μ l. All radioligand binding experiments were performed in the presence of a physiologically relevant concentration of Na⁺ (137 mM). Non-specific binding was determined with 1 μ M etorphine. Both total binding and non-specific binding curves were performed in duplicate. To reach equilibrium, reactions were incubated at 22°C with agitation for 2 h following addition of radioligand. For competition binding experiments, competing ligands were prepared in concentration-response curves in HBSS/20 mM HEPES/pH 7.4, in 96-well plates containing 10 μ g of protein per well. Then 4 nM [³H]naloxone was added to each well and binding reactions were left to incubate at 22°C for 2 h with agitation. Reaction plates were then harvested onto a 96-well filter plate using a Filtermate 96 well harvester (Perkin Elmer), with wash buffer (20mM HEPES, pH 7.4), dried for 1 h and then read on a Topcount scintillation counter (Perkin Elmer), following addition of 40 μ l of Microscint 20 scintillation fluid (Perkin Elmer) to each well.

MOL #66613

FRET experiments. Cells co-transfected with MOPr-YFP, arrestin-3-CFP and GRK2 were plated out at ~ 40% confluence on polylysine-coated glass coverslips (25 mm diameter) in 6-well plates 24 h before the experiments were performed. The coverslips were mounted on a Nikon Eclipse TE2000S inverted microscope (Nikon, Kingston, UK) using an "Attofluor" holder (Molecular Probes, Leiden, The Netherlands), and the cells were continuously superfused with HBSS using a computer-assisted solenoid valve-controlled rapid superfusion device. Ligands were also applied using the same superfusion system. Cells were observed using an oil immersion 63x lens, a polychrome V (Till Photonics, Gräfelfing, Germany) for excitation, and a dual emission photometric system (Till Photonics). To minimize photobleaching, the illumination time was set to 10–50 ms applied with a frequency of 10 Hz. Fluorescence was measured at 535 ± 15 nm (F_{535}) and 480 ± 20 nm (F_{480}) (beam splitter DCLP 505 nm, Chroma Technology, Rockingham, VT) upon excitation at 436 ± 10 nm (beam splitter DCLP 460 nm, Chroma Technology). Signals detected by avalanche photodiodes were digitized using an analog/digital converter (Digidata 1322A, Axon Instruments, Union City, CA) and stored on PC using Axoscope 9.2 software (Axon Instruments). FRET was calculated as the ratio F_{YFP}/F_{CFP} .

Receptor trafficking. Cell surface loss of MOPr was measured by enzyme-linked immunosorbent assay (ELISA) using a colorimetric alkaline phosphatase assay, as described previously (Bailey et al., 2003). In brief, HEK293 cells stably expressing T7-MOPr were first incubated with the primary antibody (anti-T7 monoclonal; 1:5000; Novagen Merck Chemicals, Nottingham,

MOL #66613

UK) for 60 min at 37°C to label surface MOPrs. Cells were then washed and incubated with opioid agonists in DMEM for 30 min at 37°C. Cells were fixed in 3.7% formaldehyde and incubated with secondary antibody (goat anti-mouse conjugated with alkaline phosphatase; 1:1000; Sigma-Aldrich, Poole, Dorset, UK), a colorimetric alkaline phosphatase substrate (Bio-Rad Laboratories, Hemel Hempstead, Herts, UK) was then added and samples were assayed at 405 nm with a microplate reader. The background was subtracted by simultaneous assay of HEK293 cells not expressing MOPr. Percentage cell surface receptor loss was calculated by normalizing data from each treatment group to corresponding control surface receptor levels determined from cells not exposed to opioid agonists. For each agonist, cell surface receptor loss was expressed as a percentage of that due to 10 µM DAMGO. All experiments were performed in triplicate.

Serine³⁷⁵ phosphorylation. HEK 293 cells stably transfected with T7-MOPr were plated onto poly-L-lysine-coated 60 mm dishes and grown to 90% confluence. Following agonist treatment for 10 min, the cells were washed with ice-cold PBS and harvested into ice-cold lysis buffer (50 mM Tris-HCl, pH 7.4, 1 mM EDTA, 120 mM NaCl, 40 mM Glycerol-2-phosphate, 1% Triton X-100, 0.5 mM Sodium Orthovanadate and the following proteinase inhibitors: 0.1 µM microcystin (Alexis Biochemicals, Exeter, UK), 4 mg/ml leupeptin, 4 mg/ml pepstatin A, 4 mg/ml antipain (all from Roche Diagnostics GmbH, Mannheim, Germany) and 4 mg/ml benzamidine, (Sigma-Aldrich, Gillingham, Dorset, UK)). The lysed cells were spun at 17,600g for 10 min at 4°C and the pellet was

MOL #66613

discarded. The T7-tagged MOPr were then immunoprecipitated by incubation in an agitation system for 2 h at 5°C with 20 µl of protein sepharose beads and 1 µl of anti-T7 monoclonal antibody (Novagen Merck Chemicals, Nottingham, UK). Immunocomplexes were precipitated, diluted in SDS sample buffer and boiled at 95°C for 4 min. The immunoprecipitated MOPrs were then submitted to electrophoresis by sodium dodecyl sulphate-polyacrylamide gel electrophoresis (SDS-PAGE). After blotting, membranes were incubated with rabbit anti-phosphoserine³⁷⁵ monoclonal antibody (1:1,000 dilution, Cell Signalling Technology, Danvers, MA) for 1 h at room temperature, followed by detection using an enhanced chemiluminescence detection system.

Films exposed to Western blot membranes were scanned, and the amount of immunoreactive signal in each lane was quantified using Scion Image software (based on NIH Image for Macintosh) from the National Institute of Health created by Wayne Rasband (Bethesda, MD, USA - available from http://www.scioncorp.com/pages/scion_image_windows.htm). Optical density (OD) units of the immunoreactive bands were obtained. In order to reduce interexperimental variability, the relative immunoreactivity of the antiphosphoserine³⁷⁵- MOPr band after different drug treatments was calculated as a percentage of the antiphosphoserine³⁷⁵- MOPr band after treatment with 10 µM DAMGO obtained from a sample loaded on the same gel. The results are expressed as mean ± S.E.M. of 3-7 independent experiments for each agonist.

Data analysis and statistics. The EC₅₀ and maximum response values for [³⁵S]GTPγS binding and arrestin-3 translocation as shown in Table 1 were

MOL #66613

determined by fitting data from individual experiments to sigmoidal concentration-response curves with variable slope in Graphpad Prism 4.0, with mean and S.E.M. calculated using individual values from each experiment.

Analysis of concentration-response data for [³⁵S]GTPγS binding and arrestin-3 recruitment using the operational model of agonism (Black and Leff, 1983) was performed in Graphpad Prism 4.0, fitting data for all agonists in a given assay simultaneously to the equation:

$$Y = E_m \cdot T^n \cdot X^n / (K+X)^n + T^n \cdot X^n$$

Here, T is tau (τ) in the operational model of agonism; X is the molar concentration of agonist; K is the equilibrium dissociation constant (K_D) and was constrained to the K_D of the agonist as determined by competition binding; E_m is the theoretical maximum response of the system and n represents a slope factor. In order to obtain values for the unknown variables E_m, τ and n, data for all agonists were fit simultaneously to this equation by non-linear regression. Both E_m and n were shared between all agonists in a given assay system, while τ was not constrained and allowed to vary for each agonist. E_m values were 1.05 for [³⁵S]GTPγS binding and 2.97 for arrestin-3 recruitment, whilst n values were 0.89 for [³⁵S]GTPγS binding and 1.76 for arrestin-3 translocation. The [³⁵S]GTPγS binding data were normalised to the maximum and minimum values evoked by DAMGO over a concentration range of 10 pM to 3 μM, as fitted to a concentration-response curve in Graphpad Prism

MOL #66613

4.0, whilst arrestin-3 recruitment data were normalised to the response evoked by 30 μ M alfentanil.

The K_D values for agonists were determined by firstly fitting competition binding data normalised to buffer (total binding) and 1 μ M etorphine (non-specific binding) to a single site competition model in Graphpad Prism 4.0. Mean and S.E.M. values for IC_{50} were then calculated from the individual values, and was used to determine K_D values for the agonists using the transformation of Cheng and Prusoff. The K_D value for [3 H]naloxone used in calculating K_D values were determined by fitting saturation binding data to a one site binding model in Graphpad Prism 4.0, with mean and S.E.M. again calculated from the individual values.

Correlation figures were produced by taking fitted values and corresponding standard errors from the respective analyses, and obtaining r^2 values for the overall correlation in Graphpad Prism 4.0. Correlations were considered to be statistically significant if $p < 0.05$.

MOL #66613

Results

Agonist-induced G protein activation. This was assessed using [³⁵S]GTP γ S binding to membranes prepared from HEK293 cells stably expressing T7-tagged MOPr, with full concentration-effect curves being obtained for twenty-two MOPr ligands. Curves for seven of the agonists (DAMGO, etorphine, norbuprenorphine, endomorphin 1, morphine, buprenorphine and meptazinol) are shown in Fig. 1A, whilst the EC₅₀ and maximum response values for all twenty-two of the agonists tested are shown in Table 1. Curves for all the agonists used are also plotted in Supplemental Data Fig. 1. The most potent agonist was etorphine (EC₅₀ 0.55 ± 0.16 nM), followed by norbuprenorphine (EC₅₀ 1.73 ± 0.70 nM). Most of the opioid drugs produced the same maximum response as DAMGO in this assay, only buprenorphine, pentazocine, meptazinol and nalorphine produced a lower maximum response. A maximum response to cyclazocine could not be obtained at the highest concentration used (100 μM).

The agonist potency order for [³⁵S]GTP γ S binding was the same when using membranes from HEK293 cells expressing the PathHunter™ system as when using membranes of HEK293 cells expressing T7-MOPr (Supplemental Data Fig. 2). This indicates that the ProLink™ moiety on the COOH-terminus of MOPr required for the arrestin-3 translocation assay (see below) does not interfere with G protein coupling.

Agonist-induced arrestin-3 recruitment using the PathHunter™ assay. Arrestin translocation was studied using HEK293 cells stably expressing MOPr tagged with ProLink™ at the COOH-terminus as well as arrestin-3 tagged

MOL #66613

at the COOH-terminus with the EA moiety. In initial experiments agonist-induced arrestin-3 recruitment induced by morphine and DAMGO increased with agonist incubation time, reaching a maximum by 2 h and declining somewhat at later times. As a consequence an agonist incubation time of 2 h was chosen for all agonists. Curves for seven of the agonists are shown in Fig. 1B, whilst the EC₅₀ and maximum response values for all the agonists tested are shown in Table 1. Curves for all the agonists used are also plotted in Supplemental Data Fig. 3. Etorphine was again the most potent agonist (EC₅₀ 6.8 ± 1.0 nM). In this assay, unlike in the [³⁵S]GTPγS assay, morphine, normorphine, 6-monoacetylmorphine (6 MAM), morphine-6-glucuronide (M6G) and levorphanol had lower maximum responses than DAMGO. The agonists that had a lower maximum response in the [³⁵S]GTPγS assay (buprenorphine, pentazocine, meptazinol and nalorphine) showed very little activity in the arrestin-3 assay. A maximum response to meperidine could not be obtained at the highest concentration used (100 μM).

Agonist-induced arrestin-3 recruitment monitored by FRET. The arrestin-3 translocation assay used above to construct full agonist concentration-effect curves was performed following agonist incubation for 2 h. Since most imaging assays of arrestin translocation normally take place following agonist addition for 30 min or less (Johnson et al., 2006), it was important to establish that the agonist-induced arrestin-3 interactions we had observed using the PathHunter™ assay system accurately reflected those that might be observed after acute agonist application. In order to do this, we employed FRET to assess MOPr/arrestin-3 interactions in the minutes following agonist application.

MOL #66613

HEK293 cells were transiently transfected with MOPr-YFP, arrestin-3-CFP, and also GRK2 (the latter being necessary to see significant FRET in this assay), and 48 h later FRET was monitored for 5 min (8 min in the case of morphine) after the addition of saturating concentrations of some MOPr agonists; in each case DAMGO (10 μ M) was added after the first drug had been washed out (see Supplemental Data Fig. 4). Addition of DAMGO, endomorphin 1, endomorphin 2 and alfentanil each produced rapid increases in the FRET ratio (Fig. 2A, B, C and D). Whilst etorphine also produced a marked increase in the FRET ratio, when the cells were washed the FRET ratio did not decrease back towards baseline as it did with the other agonists, but remained high such that no further response could be observed when DAMGO was added (Fig. 2E). Morphine produced a small increase in the FRET ratio in comparison to other agonists such as DAMGO (Fig. 2F), whilst neither buprenorphine nor pentazocine increased the FRET ratio when added to cells (Fig. 2G and H). Indeed, DAMGO was unable to produce a FRET signal after application and washout of buprenorphine an observation consistent with buprenorphine's reported partial agonist and long duration of action properties.

Together, these results demonstrate that the acute effects of opioid ligands on arrestin recruitment reflect closely those obtained following longer agonist addition in the PathHunterTM assay.

Ligand binding experiments to determine ligand K_D values at MOPr in the presence of Na^+ . In order to perform the operational analysis (see below) it was necessary to obtain K_D values for each agonist. This was done using

MOL #66613

radioligand displacement. All binding experiments were performed in HBSS buffer which contains 137 mM Na⁺. This concentration of Na⁺ is the same as that to which the receptor is exposed in the [³⁵S]GTPγS and arrestin-3 assays as well as in the study of endogenous neuronal MOPr. Na⁺ promotes binding of agonist ligands to a low affinity binding site presumed to be uncoupled from G protein (Strange, 2008).

First, saturation binding of [³H]naloxone to membranes of the HEK293 cells expressing T7-tagged MOPr was performed and the K_D of [³H]naloxone binding determined to be 1.5 ± 0.3 nM and the B_{max} was 778 ± 6 fmoles/mg protein (n=3 independent experiments). Thereafter ligand binding experiments were undertaken using 4 nM [³H]naloxone. The MOPr ligands concentration-dependently displaced [³H]naloxone binding from the membranes of HEK293 cells stably expressing T7-MOPr. Displacement curves for seven of the agonists are shown in Fig. 1C, whilst the K_D values for all the agonists are shown in Table 1. Curves for all the agonists used are plotted in Supplemental Data Fig. 5. Under the conditions used in the assay, buprenorphine and etorphine were the most potent displacers of [³H]naloxone, whilst cyclazocine and meperidine were the weakest displacers.

Saturation binding of [³H]naloxone to membranes of the PathHunter™ HEK293 cells determined that the K_D of [³H]naloxone binding was 1.2 ± 1.0 nM and the B_{max} was 282 ± 46 fmoles/mg protein (n=3 independent experiments) indicating that the MOPr expression level in the PathHunter™ cells was 36% of that in the T7-MOPr cells.

MOL #66613

Operational analysis of agonist concentration-effect curves and correlation of operational efficacy (τ) values from [35 S]GTP γ S and arrestin-3 recruitment assays. Concentration-effect curves for agonists were subjected to operational analysis as described in the Methods. Calculated τ values for each agonist in [35 S]GTP γ S and arrestin-3 assays are shown in Table 2. In both assays DAMGO and Met-enkephalin had the highest operational efficacy values. Somewhat surprisingly, the operational efficacy of etorphine for G protein activation was lower than those for six other agonists. Norbuprenorphine had much higher operational efficacy than buprenorphine for both G protein activation and arrestin-3 recruitment. Morphine, M6G and oxycodone all had similar operational efficacy values for G protein activation, and for arrestin-3 recruitment. The operational efficacy values of morphine for G protein activation and arrestin-3 recruitment were 18% and 27% of those for DAMGO, respectively. Furthermore, compared to most agonists the endomorphins had relatively high values of operational efficacy for arrestin-3 recruitment compared to operational efficacy values for G protein activation. Finally, it should be noted that operational efficacy values of arrestin-3 recruitment for six agonists could not be determined (Table 2) since responses were not detected (see Fig. 2G and H, and Supplemental Data Fig. 3), even though these compounds do have efficacy in other signalling assays (see Supplemental Data Fig. 1, also Selley et al., 1998; Borgland et al., 2003; Saidak et al., 2006).

A graph showing the correlation between operational efficacy values obtained in [35 S]GTP γ S and arrestin-3 assays is shown in Fig. 3. Correlation of

MOL #66613

the data revealed a coefficient of 0.646 ($p < 0.05$), indicating a positive correlation between relative operational efficacy for G protein activation and arrestin-3 recruitment. Inspection of the correlation also indicates that endomorphin 1 and 2 appeared to be outliers (possibly also etorphine and fentanyl) as they displayed an apparent bias towards arrestin-3 recruitment.

It was not possible to present a log-log correlation graph (see Sykes et al., 2009) between operational efficacy values obtained in [^{35}S]GTP γ S and arrestin-3 assays, for all of the agonists tested as some of the agonists had undetectable responses in the arrestin assay. Some of these agonists (e.g. buprenorphine and pentazocine) are clinically important opioids and it was considered essential to include them on the correlation plot in Fig. 3. Nevertheless, a log-log correlation for the 16 agonists with quantifiable values of operational efficacy for arrestin recruitment is included in Supplemental Data Fig. 6.

Agonist-induced phosphorylation of Serine³⁷⁵ in MOPr. Serine³⁷⁵ in the COOH-terminus tail of MOPr can be phosphorylated in an agonist-dependent fashion (Schulz et al., 2004). Using a commercially available antiphosphoserine³⁷⁵ antibody we assessed the ability of a saturating concentration of thirteen of the opioid agonists to induce phosphorylation of this residue (Fig 4). In each case, the amount of agonist-induced phosphorylation is expressed as a % of that induced by a supramaximal concentration of DAMGO (10 μM). In general the relative intrinsic activity (effect produced by a maximally effective concentration of the agonist relative to the response produced by a

MOL #66613

maximally effective concentration of an agonist that produced the greatest response) of the opioid agonists to induce phosphorylation of serine³⁷⁵ in MOPr correlated well with the operational efficacy values for arrestin-3 translocation.

Agonist-induced cell surface loss of MOPr. An ELISA technique was employed to determine the effect of a receptor saturating concentration of twenty-one of the opioid ligands on cell surface loss of MOPr, generally regarded as a reliable measure of agonist-induced GPCR internalization (Johnson et al., 2006). The results are shown in Fig 5. In each case, the amount of agonist-induced internalization is expressed as a % of that induced by a maximally effective concentration of DAMGO (10 μ M). The relative intrinsic activity of the opioid agonists to induce cell surface loss of MOPr correlated well with the operational efficacy values for arrestin-3 translocation.

MOL #66613

Discussion

This study is the first to correlate the relative intrinsic efficacy of two MOPr signalling outputs for such a wide range of opioid ligands. It shows that, for these MOPr agonists, there is a strong positive correlation between the operational efficacies for G protein activation and arrestin-3 recruitment. Previous studies have provided very useful measures of relative intrinsic activity for MOPr agonists (Traynor and Nahorski, 1995; Zaki et al., 2000; Kovoov et al., 1998; Yu et al., 1997; Saidak et al., 2006; Clark et al., 2006), however this parameter is not able to differentiate full agonists in terms of efficacy and can be highly dependent upon receptor expression levels, so for these reasons operational efficacy is a more useful measure. The operational model of agonism provides a measure of efficacy, termed operational efficacy, or τ (Black and Leff, 1983). Since τ is equal to R_T/K_e (where R_T is the receptor concentration in the tissue and K_e is the concentration of agonist-receptor complex that produces the half-maximal effect for that agonist in the tissue), then if measurements are made for a series of agonists acting at the same receptor population in a tissue, the tissue factors cancel out and the ratio of τ values become a measurement of relative intrinsic efficacy. Values of operational efficacy do not depend upon whether a particular agonist is a full or partial agonist in a tissue.

The GTP γ S concentration-response data for the MOPr agonists revealed relative potency values largely in keeping with those reported in previous studies (Traynor and Nahorski, 1995; Emmerson et al., 1996; Selley et al., 1998), with the majority of the agonists being full agonists, and etorphine being the most

MOL #66613

potent agonist (Lee et al., 1999). On the other hand a number of full agonists in the G protein assay were partial agonists in the arrestin-3 recruitment assay, including morphine, normorphine, oxycodone, M6G and 6MAM. Furthermore, the agonist EC₅₀ values obtained for arrestin-3 recruitment were all higher than the respective EC₅₀ values for G protein activation. This can be explained by a combination of there being a greater receptor reserve for G protein activation than for arrestin-3 recruitment, and a greater level of MOPr expression in the HEK293 cells used for the [³⁵S]GTPγS binding compared to the cells used for the PathHunter™ assay.

To obtain K_D values for the agonists, competition binding experiments were undertaken in the same buffer as that used for the [³⁵S]GTPγS binding and arrestin-3 recruitment experiments, containing 137 mM Na⁺. Agonist binding to some GPCRs is sensitive to the Na⁺ concentration (Strange, 2008). Such an effect was observed for MOPr function many years ago (Pert et al., 1973), and explains why the K_D values we obtained in this study are higher than many of those previously published (e.g. Selley et al., 1998).

By fitting the data from the two functional assays to the operational model, τ values of operational efficacy for [³⁵S]GTPγS binding and arrestin-3 recruitment were obtained. Overall, there was a strong positive correlation between the τ values for [³⁵S]GTPγS binding and arrestin-3 recruitment (r² = 0.649). Previous investigations of the relationship between GPCR activation and regulatory processes such as phosphorylation, desensitization and internalization have provided contrasting pictures. Whilst for some GPCRs there is a strong

MOL #66613

correlation between agonist-induced signalling and receptor phosphorylation/desensitization, for others there is a relatively poor correlation (e.g Lewis et al., 1998). However in most of these studies, relative intrinsic activity (relative maximum responses) has been used as the measure of efficacy, rather than relative operational efficacy as in the present work.

With regard to MOPr, a good correlation between receptor activation and internalization for a small series of agonists was reported (Zaki et al., 2000), whilst other studies indicated a poor correlation between MOPr activation and desensitization (Yu et al., 1997, Whistler et al., 1999). However in these latter two studies where the readout for MOPr function involved activation of G protein-gated K⁺ channels (GIRK), interpretation of the results may have been confused by the use of methadone, which can directly inhibit GIRKs (Rodriguez-Martin et al., 2008). In the current study, since GIRK activation was not used as a signalling output, then the inclusion of methadone in the analysis is not problematic.

In a detailed study (Borgland et al., 2003), the relative intrinsic efficacy of four MOPr agonists for three functional readouts (Ca²⁺ current inhibition, desensitization of Ca²⁺ current inhibition, and MOPr internalization) in the same cell type was quantified. Whilst a good correlation between MOPr activation and desensitization was reported, there was a poor correlation between MOPr activation and internalization by the agonists, principally because of the low intrinsic efficacy of morphine to induce MOPr internalization in comparison to its ability to inhibit Ca²⁺ current and promote desensitization of Ca²⁺ current

MOL #66613

inhibition. In the present study we have analysed a much wider series of MOPr agonists, and have quantified arrestin-3 recruitment rather than desensitization or internalization. Although it is reasonable to assume that arrestin-3 recruitment reflects the presence of the agonist-induced GRK/arrestin desensitization pathway, it should be borne in mind that for some agonists MOPr regulation can be largely independent of GRKs/arrestins (Chu et al., 2008; Bailey et al., 2009a; Bailey et al., 2009b), whilst on the other hand non-visual arrestins can be recruited to a GPCR to perform functions other than receptor regulation. In the present study the operational efficacy value for morphine's ability to recruit arrestin-3 to MOPr was in line with the low operational efficacy value for G protein activation, as well as the limited ability of morphine to induce MOPr internalization and Serine³⁷⁵ phosphorylation. This suggests that the lack of MOPr internalization observed with morphine in many systems (Johnson et al., 2006) can be most simply explained by the agonist's low efficacy at MOPr.

Relative to other agonists studied, endomorphin 1 and 2 (and to a lesser degree etorphine and fentanyl) are biased towards arrestin-3 recruitment. This was somewhat unexpected, as there is no previous evidence to suggest that the endomorphins induce MOPr signalling or regulation distinct from that of other agonists such as DAMGO. Indeed in some studies of MOPr signalling outputs the endomorphins appear to be partial agonists (e.g. Saidak et al., 2006). One possibility is that different agonists stabilize distinct active conformations of MOPr, which consequently have varying affinities for G protein and GRK/arrestins. This phenomenon, termed functional selectivity (Urban et al.,

MOL #66613

2007), has now been observed with particular agonists at a number of different GPCRs (Sanchez-Blazquez et al., 2001). Whether or not the endomorphins can stabilize an active conformation of MOPr that is distinct from, for example, Met-Enkephalin or DAMGO, remains to be determined.

Apart from the effects of the endomorphins, another somewhat unexpected feature of the present data was that the operational efficacy of etorphine for G protein activation was only around half that for Met-Enkephalin or DAMGO. Interestingly preliminary recordings of MOPr agonist-induced K⁺ channel activation in locus coeruleus neurones contained in slices of rat brainstem also indicate that etorphine has lower operational efficacy than DAMGO (unpublished observations). Etorphine is a full agonist at MOPr in all systems studied (Clark et al., 2006), and because of its high potency is generally considered to possess high efficacy at MOPr. However our results indicate that etorphine's high potency is due principally to a very high affinity for MOPr (Lee et al., 1999). This underlines the importance of obtaining measures of relative intrinsic efficacy when comparing agonist efficacy.

Finally, in this study we also assessed the ability of some agonists to induce either MOPr internalization or phosphorylation of Serine³⁷⁵ in the COOH-terminus of MOPr. There was a good correlation between the intrinsic activity for agonist-induced Serine³⁷⁵ phosphorylation and operational efficacy values for arrestin-3 recruitment, and also between the intrinsic activity for internalization and operational efficacy values for arrestin-3 recruitment. Since for most GPCRs, GRK-mediated phosphorylation is considered to be an important step in arrestin

MOL #66613

recruitment, and since arrestin binding to most GPCRs is important for efficient internalization (Kelly et al., 2007), then the high degree of correlation between these measures is not unexpected.

In conclusion this study demonstrates that, apart from a handful of agonists that include the endomorphins, MOPr agonists display a good correlation between the operational efficacy for G protein activation and the operational efficacy for non-visual arrestin recruitment. Future studies will be directed towards determining whether an enhanced interaction of arrestins with the endomorphin 1- or endomorphin 2-occupied MOPr has particular functional consequences. Morphine's limited ability to induce MOPr internalization in most systems can be explained by its low efficacy for MOPr signalling. We have previously suggested that for morphine, desensitization and tolerance are mediated in large part by PKC whereas for DAMGO, an agonist of high operational efficacy, desensitization and tolerance are mediated by GRK (Johnson et al., 2006; Bailey et al., 2009b; Hull et al., 2010). It will be important to determine whether for the majority of MOPr agonists the mechanism of desensitization (PKC versus GRK/arrestin) is simply a function of efficacy for G protein activation.

MOL #66613

References

- Bailey CP, Couch D, Johnson E, Griffiths K, Kelly E, and Henderson G (2003) μ -Opioid receptor desensitization in mature rat neurons: lack of interaction between DAMGO and morphine. *J Neurosci* **23**:10515-10520.
- Bailey CP, Connor M (2005) Opioids: Cellular mechanisms of tolerance and physical dependence. *Curr Opin Pharmacol* **5**: 60-68.
- Bailey CP, Smith FL, Kelly E, Dewey WL and Henderson G (2006) How important is protein kinase C α in opioid receptor desensitization and morphine tolerance? *Trends Pharmacol Sci* **27**: 558-565.
- Bailey CP, Llorente J, Gabra BH, Smith FL, Dewey WL, Kelly E and Henderson G (2009a) Role of Protein Kinase C and μ -opioid receptor (MOPr) desensitization in tolerance to morphine in rat locus coeruleus neurons. *Eur J Neurosci* **29**:307-318.
- Bailey CP, Oldfield S, Llorente J, Caunt CJ, Teschemacher AG, Roberts L, McArdle CA, Smith FL, Dewey WL, Kelly E and Henderson G (2009b) Role of PKC α and G-protein-coupled receptor kinase 2 in agonist-selective desensitization of μ -opioid receptors in mature brain neurones. *Br J Pharmacol* **158**: 157-164.
- Black JW and Leff P (1983) Operational models of pharmacological agonism. *Proc R Soc Lond B Biol Sci* **220**:141-162.
- Borgland SL, Connor M, Osborne PB, Furness JB and Christie MJ (2003) Opioid agonists have different efficacy profiles for G protein activation, rapid

MOL #66613

desensitization, and endocytosis of μ -opioid receptors. *J Biol Chem* **278**: 18776-18784.

Christie MJ (2008) Cellular neuroadaptations to chronic opioids: tolerance, withdrawal and addiction. *Br J Pharmacol* **154**: 384-396.

Christopoulos A and El-Fakahany EE (1999) Qualitative and quantitative assessment of relative agonist efficacy. *Biochem Pharmacol* **58**: 735-748.

Chu J, Zheng H, Loh HH, and Law P-Y (2008) Morphine-induced μ -opioid receptor rapid desensitization is independent of receptor phosphorylation and β -arrestins. *Cell Signalling* **20**: 1616-1624.

Clark MJ, Furman CA, Gilson TD and Traynor JR (2006) Comparison of the relative efficacy and potency of μ -opioid agonists to activate $G\alpha_{i/o}$ proteins containing a pertussis toxin-insensitive mutation. *J Pharmacol Exp Therap* **317**: 858-864.

Connor M, Osborne PB and Christie MJ (2004) μ -opioid receptor desensitization: Is morphine different? *Brit J Pharmacol* **143**: 685-696.

Corbett AD, Henderson G, McKnight AT, and Paterson SJ (2006) 75 years of opioid research: the exciting but vain quest for the Holy Grail. *Br J Pharmacol* **147**: S153-S162.

Duttaroy A and Yoburn BC (1995) The effect of intrinsic efficacy on opioid tolerance. *Anesthesiol* **82**: 1226-1236.

Emmerson PJ, Clark MJ, Mansour A, Akil H, Woods JH and Medzihradsky F (1996) Characterization of opioid agonist efficacy in a C_6 glioma cell line expressing the μ opioid receptor. *J Pharmacol Exp Therap* **278**: 1121-1127.

MOL #66613

Furchgott RF and Bursztyn P (1967) Comparison of dissociation constants and of relative efficacies of selected agonists acting on parasympathetic receptors.

Ann NY Acad Sci **144**: 882-898.

Grecksch G, Bartzsch K, Widera A, Becker A, Hollt V and Koch T (2006) Development of tolerance and sensitization to different opioid agonists in rats.

Psychopharmacol **186**: 177-184.

Hull LC, Llorente J, Gabra BH, Smith FL, Kelly E, Bailey CP, Henderson G, and Dewey WL (2010) The effect of protein kinase C and G protein-coupled receptor kinase inhibition on tolerance induced by μ -opioid agonists of different efficacy.

J Pharmacol Exp Ther **332**: 1127-1135.

Johnson EA, Oldfield S, Braksator E, Gonzalez-Cuello A, Couch D, Hall KJ, Mundell SJ, Bailey CP, Kelly E, and Henderson G (2006) Agonist-selective mechanisms of μ -opioid receptor desensitization in human embryonic kidney 293 cells.

Mol Pharmacol **70**:676-685.

Kelly E, Bailey CP, and Henderson G (2007) Agonist-selective mechanisms of GPCR desensitization.

Br J Pharmacol **153**: S379-S388.

Koch T and Hollt V (2008) Role of receptor internalization in opioid tolerance and dependence.

Pharmacol Therap **117**: 199-206.

Kovoor A, Celver JP, Wu A, and Chavkin C (1998) Agonist induced homologous desensitization of μ -opioid receptors mediated by G proteibn-coupled receptor kinases is dependent on agonist efficacy.

Mol Pharmacol **54**: 704-711.

MOL #66613

Krasel C, Bunemann M, Lorenz K, and Lohse MJ (2005) β -Arrestin binding to the β_2 -adrenergic receptor requires both receptor phosphorylation and receptor activation. *J Biol Chem* **280**: 9528-9535.

Lee KO, Akil H, Woods JH, and Traynor JR (1999) Differential binding properties of oripavines at cloned μ - and δ -opioid receptors. *Eur J Pharmacol* **378**: 323–330.

Lewis MM, watts VJ, Lawler CP, Nichols DE and Mailman RB (1998) Homologous desensitization of the D_{1A} dopamine receptor: Efficacy in causing desensitization dissociates from both receptor occupancy and functional potency. *J Pharmacol Exp Therap* **286**: 345-353.

Martini L and Whistler JL (2007) The role of μ opioid receptor desensitization and endocytosis in morphine tolerance and dependence. *Curr Opin Neurobiol* **17**: 556-564.

Pert CB, Pasternak G and Snyder SH (1973) Opiate agonists and antagonists discriminated by receptor binding in brain. *Science*. **182**:1359-1361.

Rodriguez-Martin I, Braksator E, Bailey CP, Goodchild S, Marrion NV, Kelly E, and Henderson G (2008) Methadone: does it really have low efficacy at μ -opioid receptors? *Neuroreport* **19**: 589-593.

Saidak Z, Blake-Palmer K, Hay DL, Northup JK, and Glass M (2006) Differential activation of G proteins by μ -opioid receptor agonists. *Br J Pharmacol* **147**: 671-680.

MOL #66613

Sanchez-Blazquez P, Gomez-Serranillos P, and Garzon J (2001) Agonists determine the pattern of G-protein activation in μ -opioid receptor-mediated supraspinal analgesia. *Brain Res Bull* **54**: 229-235.

Schulz S, Mayer D, Pfeiffer M, Stumm R, Koch T and Holtt V (2004) Morphine induces terminal μ -opioid receptor desensitization by sustained phosphorylation of serine-375. *EMBO J* **23**: 3282-3289.

Selley DE, Liu Q and Childers SR (1998) Signal transduction correlates of μ opioid agonist intrinsic efficacy: Receptor-stimulated [³⁵S]GTP γ S binding in mMOR-CHO cells and rat thalamus. *J Pharmacol Exp Therap* **285**: 496-505.

Strange PG (2008) Agonist binding, agonist affinity and agonist efficacy at G protein-coupled receptors. *Br J Pharmacol* **153**: 1353-1363.

Sykes DA, Dowling MR and Charlton SJ (2009) Exploring the mechanism of agonist efficacy: a relationship between efficacy and agonist dissociation rate at the muscarinic M₃ receptor. *Mol Pharmacol* **76**: 543-551.

Traynor JR and Nahorski SR (1995) Modulation by μ -opioid agonists of Guanosine-5'-O-(3-[³⁵S]thio)triphosphate binding to membranes from human neuroblastoma SH-SY5Y cells. *Mol Pharmacol* **47**: 848-854.

Urban JW, Clarke WP, von Zastrow M, Nichols DE, Kobilka B, Weinstein H, Javitch, JA, Roth BL, Christopoulos A, Sexton PM, Miller KJ, Spedding M, and Mailman RB (2007) Functional selectivity and classical concepts of quantitative pharmacology. *J Pharmacol Exp Ther* **320**:1-13.

MOL #66613

Whistler JL, Chuang H-H, Chu P, Jan LY, and von Zastrow M (1999) Functional dissociation of μ opioid receptor signalling and endocytosis: Implications for the biology of opiate tolerance and addiction. *Neuron* **23**: 737-746.

Williams JT, Christie MJ, and Manzoni O (2001) Cellular and synaptic adaptations mediating opioid dependence. *Physiol Rev* **81**: 299-343.

Yu Y, Zhang L, Yin X, Sun H, Uhl GR and Wang JB (1997) μ Opioid receptor phosphorylation, desensitization, and ligand efficacy. *J Biol Chem* **272**: 28869-28874.

Zaki PA, Keith DE Jr, Brine GA, Carroll FI and Evans CJ (2000) Ligand-induced changes in surface μ -opioid receptor number: relationship to G protein activation? *J Pharmacol Exp Therap* **292**:1127-34.

MOL #66613

Footnotes

This work was supported by the Medical Research Council [Grant G0600943] , the National Institute on Drug Abuse [Grant DA 020836] and the Biotechnology and Biochemical Sciences Research Council [Grant BB/D012902/1] .

Present addresses: ¹Department of Pharmacology and Toxicology, Kuwait University, PO Box 2493, Safat 13110, Kuwait (S.A.) and ²School of Pharmacy, Dept. of Pharmacology, Karl-von-Frisch-Str. 1, 35043 Marburg, Germany (C.K.)

MOL #66613

Legends for Figures

Fig. 1. MOPr agonist concentration-effect curves. Data were obtained in HEK293 cells for (A) [³⁵S]GTP γ S binding to membranes, (B) arrestin-3 recruitment in intact cells using the PathHunterTM assay, and (C) displacement of [³H]naloxone from membranes. The same seven agonists are included on each of the three sets of axes, and in each graph the mean data for each agonist have been fitted to a sigmoidal concentration response curve with variable slope. Values are means \pm S.E.M. from 3-6 independent experiments.

Fig. 2. Interaction of MOPr with arrestin-3 as measured by FRET. HEK293 cells were transiently transfected with rat MOPr-YFP, GRK2 and Arrestin-3-CFP. In order to compare FRET responses between experiments, all drug applications (indicated by the horizontal bars) were followed by an application of 10 μ M DAMGO. An increase in the FRET ratio (measured as F_{535}/F_{480}) reflects the interaction between MOPr-YFP and Arrestin 3-CFP. Traces were filtered off-line with Axoscope 9.2. FRET traces were also corrected for photobleaching by converging the first 120 sec to a one-phase exponential decay equation, with the exception of the morphine trace which was manually adjusted by Axoscope 9.2. The absolute increase in FRET signal for each agonist varied between experiments, with a consequent increase in noise for smaller responses (e.g. B versus A). Data shown are representative of at least three independent

MOL #66613

experiments. An example of DAMGO-induced changes in F_{535}/F_{480} is shown in Supplemental data Fig. 4.

Fig. 3. Correlation of operational efficacy (τ) values for MOPr agonist-induced [35 S]GTP γ S binding and arrestin-3 recruitment in HEK293 cells.

Linear regression of data points revealed an r^2 value of 0.649 ($p < 0.05$); the dotted lines denote the 95% confidence intervals for the regression. The τ values shown are the fitted values from operational analysis of all data \pm standard error of the fitted value.

Fig. 4. Agonist-induced phosphorylation of Serine³⁷⁵ in the COOH-terminus of MOPr detected with an antiphosphoserine³⁷⁵ antibody. (A) Examples of Western blots showing phosphorylation of Serine³⁷⁵ by receptor saturating concentrations of different MOPr agonists. (B) Phosphorylation of Serine³⁷⁵ induced by thirteen MOPr agonists, normalised to that induced by DAMGO (10 μ M). Values are means \pm S.E.M. from at least 3 different experiments. The agonist concentration was 10 μ M for etorphine, buprenorphine, met-enkephalin, leu-enkephalin, fentanyl and alfentanil, and 30 μ M for all other agonists. (C) Correlation of agonist intrinsic activity for Serine³⁷⁵ phosphorylation with operational efficacy (τ) values for [35 S]GTP γ S binding. Linear regression of the data revealed an r^2 value of 0.299. Phosphorylation values are expressed as means \pm S.E.M., whilst the τ values for [35 S]GTP γ S binding are the fitted values from operational analysis of all data \pm standard error of the fitted values. (D)

MOL #66613

Correlation of agonist intrinsic activity for Serine³⁷⁵ phosphorylation with τ values for arrestin-3 recruitment. Linear regression of the data revealed an r^2 value of 0.797. MOPr phosphorylation values are expressed as means \pm S.E.M., whilst τ values for arrestin-3 recruitment are the fitted values from operational analysis of all data \pm standard error of the fitted values. The dotted lines in (C) and (D) denote the 95% confidence intervals for the regression.

Fig. 5. Agonist-induced internalization of MOPr. MOPr internalization was measured by ELISA. (A) Internalization of MOPr in response to saturating concentrations of agonist, normalised to that induced by DAMGO (10 μ M). Agonist was applied for 30 min, which produced maximum cell surface loss of MOPr for DAMGO. Values are means \pm S.E.M. from at least 3 different experiments. The agonist concentration was 10 μ M for etorphine, met-enkephalin, leu-enkephalin, buprenorphine, fentanyl, alfentanil and cyclazocine, and 30 μ M for the other agonists. (B) Correlation of agonist intrinsic activity for agonist-induced cell surface loss with operational efficacy (τ) values for [³⁵S]GTP γ S binding. Linear regression revealed an r^2 value of 0.597. Internalization values are expressed as means \pm S.E.M., whilst the τ values for [³⁵S]GTP γ S binding are the fitted values from operational analysis of all data \pm standard error of the fitted values. (C) Correlation of intrinsic activity for agonist-induced cell surface loss with operational efficacy (τ) values for arrestin-3 recruitment. Linear regression revealed an r^2 value of 0.739. Internalization values are expressed as means \pm S.E.M., whilst the τ values for arrestin-3

MOL #66613

recruitment are the fitted values from operational analysis of all data \pm standard error of the fitted values. The dotted lines in (B) and (C) denote the 95% confidence intervals for the regression.

MOL #66613

Tables

Table 1. Comparison of potency and maximum response of agonist-induced [³⁵S]GTP γ S binding and arrestin-3 recruitment for twenty-two opioid agonists acting at MOPr in HEK293 cells. Agonists are positioned in the table according to potency in the [³⁵S]GTP γ S binding assay, the most potent agonist (etorphine) being positioned at the top. Also shown are K_D values for the agonists as determined in [³H]naloxone competition binding experiments. ^a Maximum [³⁵S]GTP γ S response for each agonist expressed relative to that obtained for DAMGO (taken as 1). ^b Maximum arrestin-3 recruitment response for each agonist expressed relative to alfentanil (taken as 1). ^c Values for these agonists determined from a curve fitted to the mean data, as it was not possible to obtain fits of individual curves. ^d Estimation since maximum response was not obtained at the highest concentration of agonist used. (–) indicates where it was not possible to determine values as maximum agonist response not obtained, or due to lack of significant response at highest agonist concentrations used. Apart from the exceptions detailed above, values represent mean \pm S.E.M. of at least 3 independent experiments for each agonist.

MOL #66613

Agonist	³⁵ S]GTPγS binding		Arrestin-3 recruitment		K _D (nM)
	EC ₅₀ (nM)	Max response ^a	EC ₅₀ (nM)	Max response ^b	
Etorphine	0.55 ± 0.16	0.92 ± 0.06	6.8 ± 1.0	1.22 ± 0.08	3.5 ± 0.3
Norbuprenorphine	1.7 ± 0.7	0.93 ± 0.02	84.6 ± 12.1	1.16 ± 0.09	24.6 ± 4.5
Met-enkephalin	7.7 ± 1.9	0.88 ± 0.06	939 ± 325	1.38 ± 0.16	281 ± 13
DAMGO	11.2 ± 1.93	1.04 ± 0.02	414 ± 90	1.24 ± 0.09	228 ± 74
Buprenorphine	14.5 ± 5.11	0.55 ± 0.04	-	-	0.9 ± 0.1
Leu-enkephalin	30.9 ± 12.0	0.87 ± 0.05	5160 ± 1490	0.94 ± 0.10	744 ± 84
Levorphanol	33.1 ± 17.2	0.98 ± 0.11	265 ± 112	0.24 ± 0.03	23.2 ± 2.2
Fentanyl	56.8 ± 31.2	1.14 ± 0.11	210 ± 42	0.89 ± 0.13	158 ± 24
Pentazocine	77.9 ^c	0.26 ^c	-	-	149 ± 27
6MAM	73.3 ± 26.1	0.96 ± 0.03	1540 ± 700	0.45 ± 0.07	318 ± 86
M6G	81.0 ± 27.7	0.87 ± 0.06	1600 ± 370	0.27 ± 0.05	437 ± 227
Methadone	87.2 ± 42.2	1.18 ± 0.09	2110 ± 999	1.14 ± 0.16	552 ± 81
Alfentanil	90.3 ± 16.2	0.99 ± 0.01	638 ± 192	1.01 ± 0.16	866 ± 156
Morphine	97.5 ± 28.5	0.98 ± 0.03	322 ± 44	0.19 ± 0.03	250 ± 52
Endomorphin 2	138 ± 31	1.04 ± 0.04	311 ± 121	1.22 ± 0.01	283 ± 54
Endomorphin 1	183 ± 96	1.11 ± 0.11	226 ± 43	0.95 ± 0.04	281 ± 31
Normorphine	259 ± 165	1.11 ± 0.14	768 ± 165	0.52 ± 0.09	578 ± 141
Meptazinol	289 ^c	0.38 ^c	-	-	462 ± 71
Oxycodone	564 ± 195	0.95 ± 0.12	1460 ± 1290	0.18 ± 0.03	1550 ± 328
Meperidine	>10,000 ^d	-	-	-	7110 ± 3300
Cyclazocine	>10,000 ^d	-	-	-	17500 ± 725
Nalorphine	>10,000 ^d	-	-	-	13.1 ± 0.6

MOL #66613

Table 2. Calculated operational efficacy (τ) values for [^{35}S]GTP γ S binding and arrestin-3 recruitment for twenty-two opioid agonists. Data were fitted to the operational model of pharmacological agonism as described in the Methods. Values are arranged in order of magnitude of the τ value for [^{35}S]GTP γ S binding, with the highest (DAMGO) at the top. (-) denotes where it was not possible to determine τ values as either a maximum response to the agonist could not be obtained at the highest concentration of agonist used, or the maximum response produced by the agonist was too small, or a response was undetectable. Each agonist concentration-effect curve was repeated at least 3 times; the τ values shown are the fitted values from operational analysis of all data \pm standard error of the fitted value.

MOL #66613

Agonist	Operational efficacy (τ)	
	[³⁵ S]-GTP γ S	Arrestin-3 recruitment
DAMGO	28.5 \pm 1.1	0.82 \pm 0.08
Met-enkephalin	22.0 \pm 1.1	0.86 \pm 0.20
Methadone	18.2 \pm 0.9	0.67 \pm 0.04
Leu-enkephalin	14.2 \pm 0.9	0.56 \pm 0.08
Norbuprenorphine	13.9 \pm 0.8	0.71 \pm 0.05
Fentanyl	12.3 \pm 0.6	0.64 \pm 0.08
Etorphine	11.3 \pm 0.5	0.80 \pm 0.09
Alfentanil	10.7 \pm 0.6	0.76 \pm 0.06
Normorphine	8.8 \pm 0.4	0.44 \pm 0.06
6MAM	6.6 \pm 0.3	0.36 \pm 0.03
Endomorphin 1	6.2 \pm 0.2	0.71 \pm 0.05
M6G	5.2 \pm 0.2	0.25 \pm 0.01
Morphine	5.2 \pm 0.2	0.22 \pm 0.01
Oxycodone	5.1 \pm 0.2	0.23 \pm 0.01
Endomorphin 2	5.1 \pm 0.2	0.84 \pm 0.08
Levorphanol	3.7 \pm 0.1	0.21 \pm 0.01
Buprenorphine	0.6 \pm 0.1	-
Meptazinol	0.5 \pm 0.1	-
Pentazocine	0.3 \pm 0.1	-
Meperidine	-	-
Cyclazocine	-	-
Nalorphine	-	-

MOL #66613

Figures

Fig 1

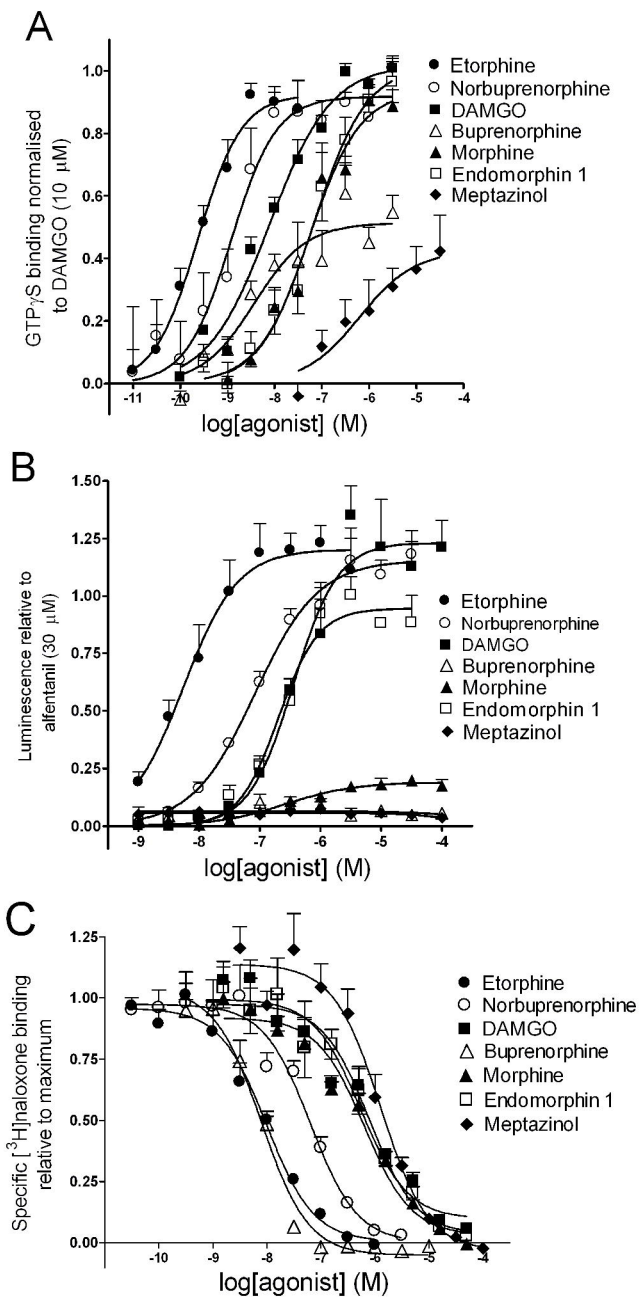


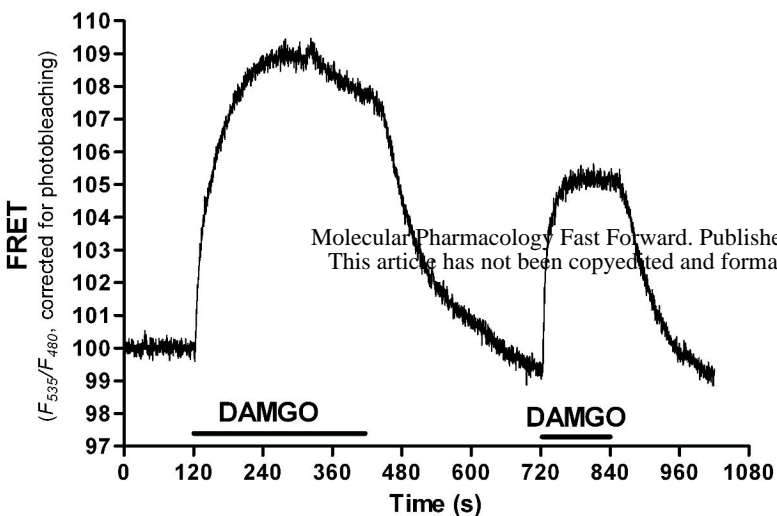
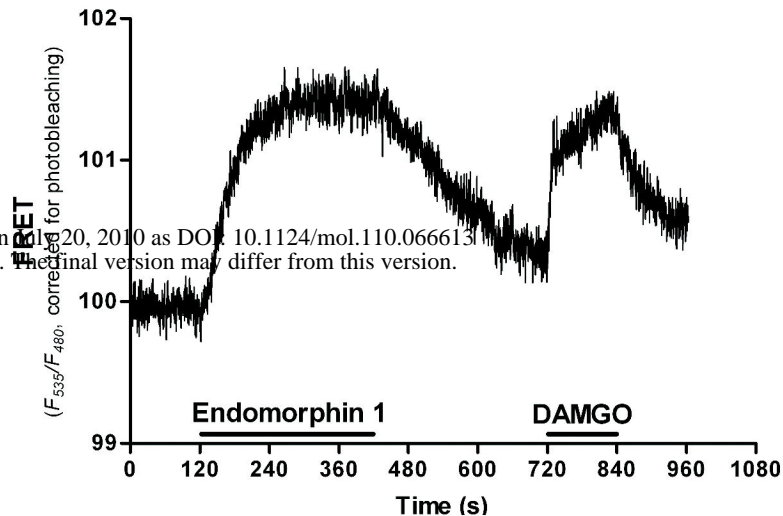
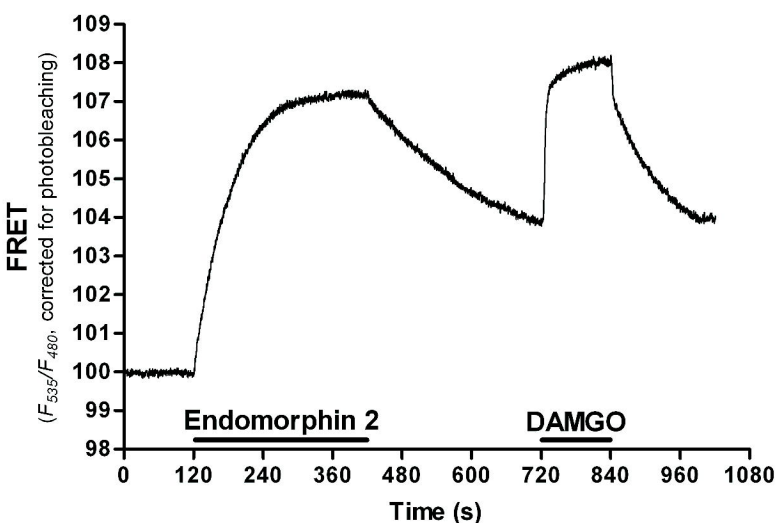
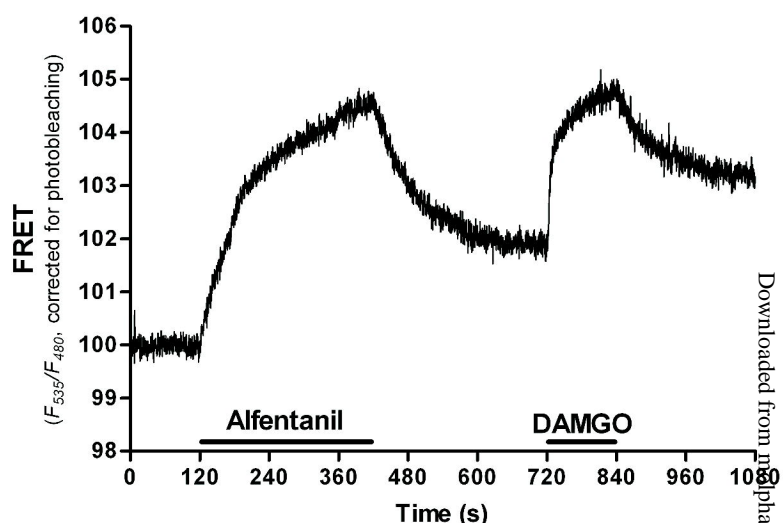
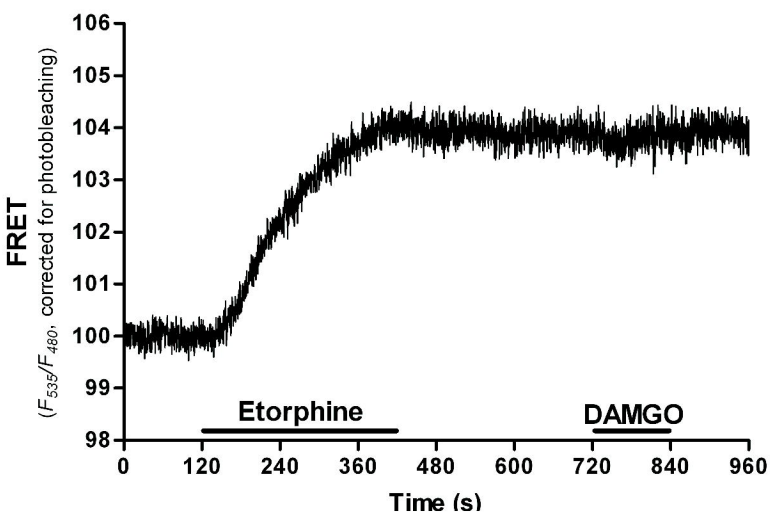
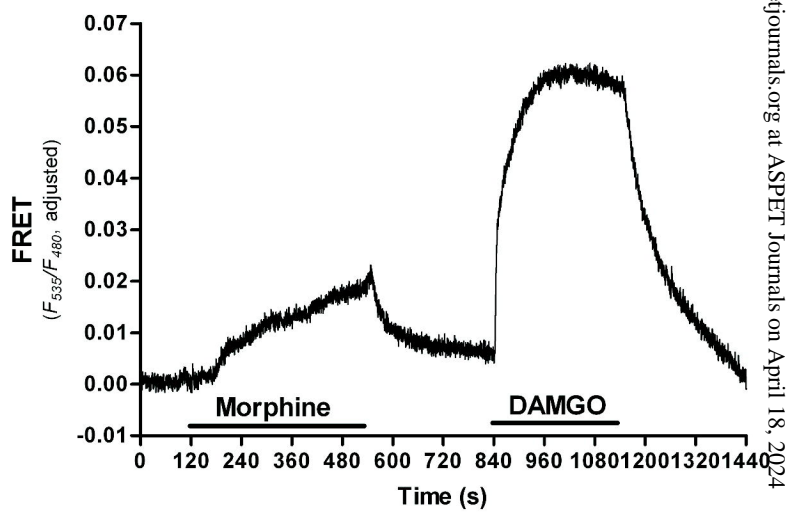
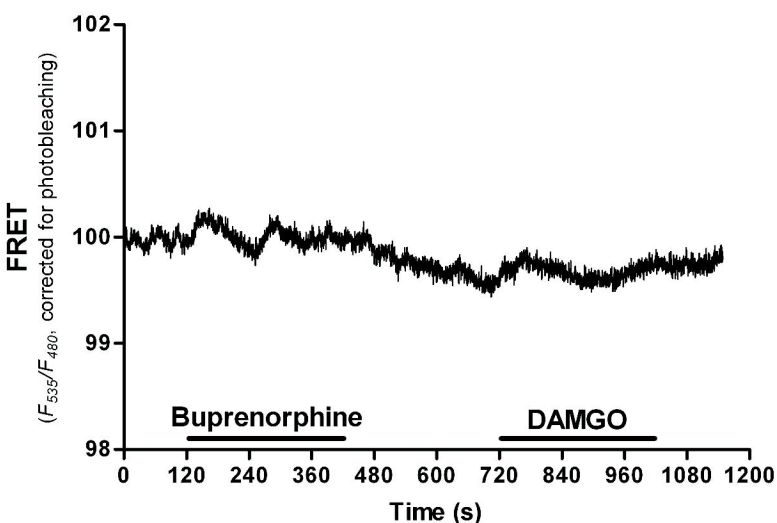
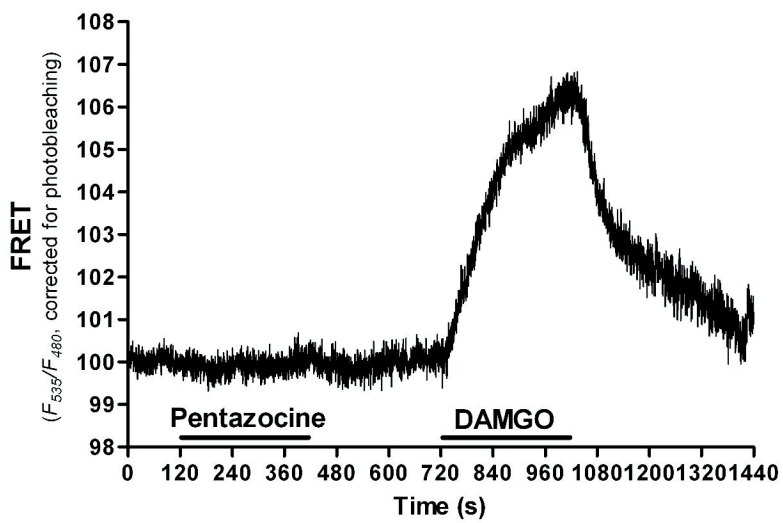
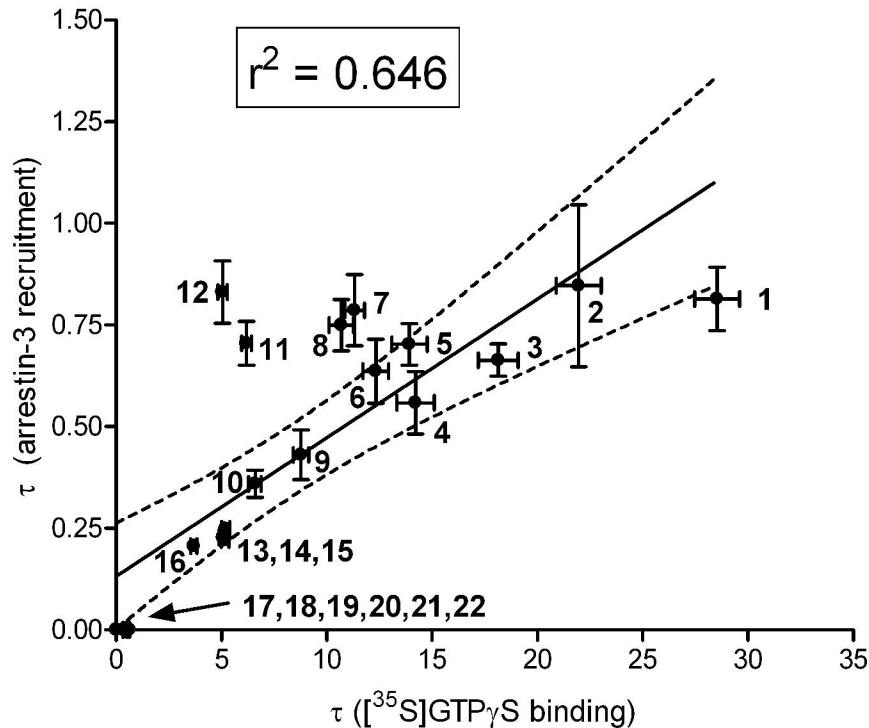
Fig. 2**A****DAMGO 10 μ M****B****Endomorphin 1 30 μ M****C****Endomorphin 2 30 μ M****D****Alfentanil 10 μ M****E****Etorphine 10 μ M****F****Morphine 30 μ M****G****Buprenorphine 10 μ M****H****Pentazocine 30 μ M**

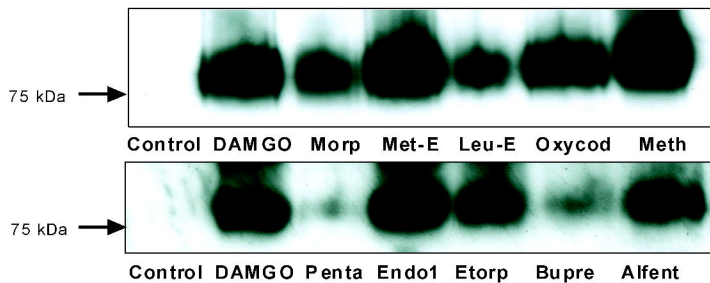
Fig 3



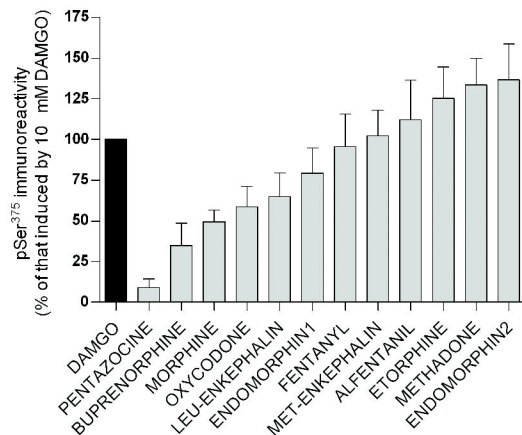
- 1 DAMGO
- 2 Met Enkephalin
- 3 Methadone
- 4 Leu Enkephalin
- 5 Norbuprenorphine
- 6 Fentanyl
- 7 Etorphine
- 8 Alfentanil
- 9 Normorphine
- 10 6MAM
- 11 Endomorphin1
- 12 Endomorphin2
- 13 Oxycodone
- 14 Morphine
- 15 M6G
- 16 Levorphanol
- 17 Meperidine
- 18 Cyclazocine
- 19 Buprenorphine
- 20 Meptazinol
- 21 Pentazocine
- 22 Nalorphine

Fig. 4

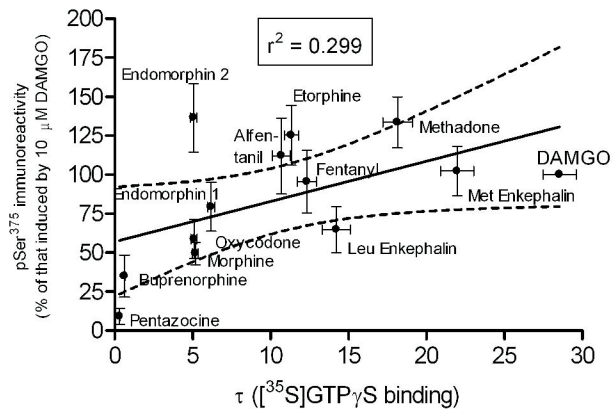
A



B



C



D

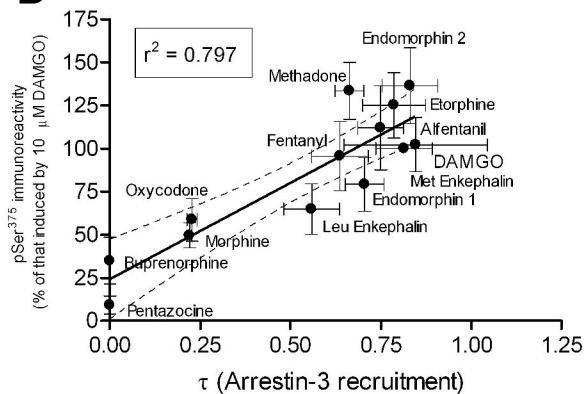
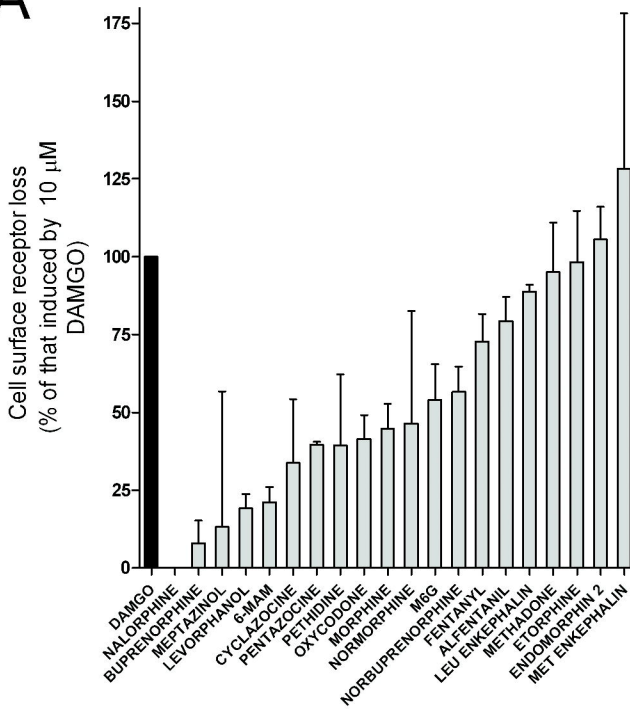
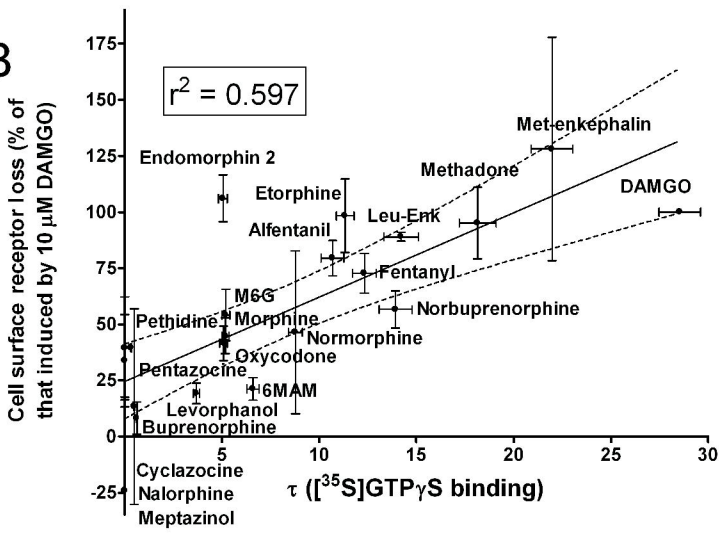


Fig. 5

A



B



C

